Inorg. Chem. **2008**, *47*, 7483−7492

Syntheses, Structures, and Photophysical Properties of Mono- and Dinuclear Sulfur-Rich Gold(I) Complexes

Fabrice Guyon,*,† Aurélien Hameau,† Abderrahim Khatyr,† Michael Knorr,† Hedi Amrouche,‡ Daniel Fortin,‡ Pierre D. Harvey,*,‡ Carsten Strohmann,§ Amadou L. Ndiaye,†,|| Volker Huch,|| Michael Veith,||,⊥ and Narcis Avarvari#

Institut UTINAM, UMR CNRS 6213, Université de Franche-Comté, Faculté des Sciences et Techniques, 16 route de Gray, 25030 Besançon, France, Département de Chimie, Université de Sherbrooke, Sherbrooke, J1K 2R1 Québec, Canada, Institut für Anorganische Chemie der Universität Würzburg, Am Hubland, D-97074 Würzburg, Germany, INM-Leibniz Institute for New Materials, Campus D2 2, Saarland University, Im Stadtwald, Gebäude D2 2, 66123 Saarbrücken, Germany, Institute for Inorganic Chemistry, Saarland University, PO Box 15 11 50, 66041 Saarbruecken, Germany, and Laboratoire ≪ Chimie Ingénierie Moléculaire et Matériaux ≫ (CIMMA), UMR 6200, 2 boulevard Lavoisier, 49045 Angers, France

Received November 9, 2007

The dinuclear gold complexes [{Au(PPh_3)}$_2$(μ-*dmid*)] (**1**) (*dmid* = 1,3-dithiole-2-one-4,5-dithiolate) and [{Au(PPh_3)}$_2$(μ-*dddt*)] (**2**) (*dddt* = 5,6-dihydro-1,4-dithiine-2,3-dithiolate) were synthesized and characterized by X-ray crystallography. Both complexes exhibit intramolecular aurophilic interactions with Au···Au distances of 3.1984(10) Å for **1** and 3.1295(11) Å for **2**. A self-assembly reaction between 4,5-bis(2-hydroxyethylthio)-1,3-dithiole-2-thione (*(HOCH$_2$CH$_2$)$_2$dmit*) and [AuCl(tht)] affords the complex [AuCl{*(HOCH$_2$CH$_2$)$_2$dmit*}]$_2$ (**4**), which possesses an antiparallel dimeric arrangement resulting from a short aurophilic contact of 3.078(6) Å. This motif is extended into two dimensions due to intra- and intermolecular hydrogen bonds via the hydroxyethyl groups, giving rise to a supramolecular network. Three compounds were investigated for their rich photophysical properties at 298 and 77 K in 2-MeTHF and in the solid state; [Au$_2$(μ-*dmid*)(PPh_3)$_2$] (**1**), [Au$_2$(μ-*dddt*)(PPh_3)$_2$] (**2**), and [AuCl{(*HOCH$_2$CH$_2$)$_2$dmit*}] (**4**). **1** exhibits relatively long-lived LMCT (ligand-to-metal charge transfer) emissions at 298 K in solution (370 nm; τ_e ∼17 ns, where M is a single gold not interacting with the other gold atom; i.e., the fluxional C-SAuPPh_3 units are away from each other) and in the solid state (410 nm; τ_e ∼70 μs). At 77 K, a new emission band is observed at 685 nm (τ_e = 132 μs) and assigned to a LMCT emission where M is representative for two gold atoms interacting together consistent with the presence of Au···Au contacts as found in the crystal structure. In solution at 77 K, the LMCT emission is also red-shifted to 550 nm (τ_e ∼139 μs). It is believed to be associated to a given rotamer. **2** also exhibits LMCT emissions at 380 nm at 298 K in solution and at 470 nm in the solid state. **4** exhibits X/MLCT emission (halide/metal to ligand charge transfer) where M is a dimer in the solid state with obvious Au···Au interactions, resulting in red-shifted emission band, and is a monomer in solution in the 10^{-5} M concentration (i.e., no Au···Au interactions) resulting in blue-shifted luminescence. Both fluorescence and phosphorescence are observed for **4**.

Introduction

Di- and polynuclear gold complexes have attracted much attention in the past two decades due to the rich luminescence properties generally associated with these systems.[1] It was recognized that aurophilic Au···Au contacts may play a central role in the photophysical properties of gold(I) complexes.[2] For example, Yam and colleagues have developed luminescence chemosensors based on the switching on and off of weak Au···Au interactions using dinuclear gold(I) phosphine thiolate complexes.[3] Numerous studies were devoted to the synthesis of complexes which exhibit inter- or intramolecular metal−metal interactions. Of particular

* To whom correspondence should be addressed. E-mail: fabrice.guyon@univ-fcomte.fr.
† Université de Franche-Comté, Faculté des Sciences et Techniques.
‡ Département de Chimie, Université de Sherbrooke.
§ Institut für Anorganische Chemie der Universität Würzburg.
|| INM-Leibniz Institute for New Materials.
⊥ Institute for Inorganic Chemistry, Saarland University.
Laboratoire ≪ Chimie Ingénierie Moléculaire et Matériaux ≫.

10.1021/ic7022067 CCC: $40.75
Published on Web 07/29/2008

interest are the dithiolene compounds for the following reasons: (i) as soft Lewis bases, the electrochemically active dithiolene ligands possess a high affinity toward gold, (ii) because they may act as bridging ligands, they promote the formation of dinuclear gold complexes with intramolecular Au···Au separations shorter than the sum of the Van der Waals radii of gold. Moreover, (iii) some of them may favor intermolecular contacts via S···S interaction.[4] The family of 1,2 dithiolene ligands includes sulfur-rich dithiolenes, such as 1,3-dithiole-2-thione-4,5-dithiolate (*dmit*), which was successfully used for nickel, palladium, or platinum complexes for the elaboration of conducting and superconducting molecular materials.[5] The remarkable properties of these synthetic metals result mainly from the propensity of the ligand to overlap with each other in the solid state due to the presence of numerous sulfur atoms. Also, some [$(AuL)_2(\mu$-dmit)] (L = phosphane) complexes[6] and related derivatives[7] were reported and structurally characterized. However, there are no thorough reports on their photophysical properties. In continuation of our previous studies on dithiolene complexes,[8] we wish to report the synthesis, structural characterization, and photophysical studies of two novel sulfur-rich dithiolene gold(I) complexes based on the 1,3-dithiole-2-one-4,5-dithiolate (*dmid*) and the more electron-rich 5,6-dihydro-1,4-dithiine-2,3-dithiolate (*dddt*) ligands, as well as the compounds resulting from the self-assembly processes between 4,5-bis(methylthio)-1,3-dithiole-2-thione (*Me_2dmit*) or 4,5-bis(2-hydroxyethylthio)-1,3-dithiole-2-thione (*$(HOCH_2CH_2)_2$dmit*) ligands and the [AuCl] fragment. This second approach was motivated by the recent syntheses of the coordination polymers $[HgX_2(Me_2dmit)]_n$ (X = Cl, Br, I),[9] $[CuX(Me_2dmit)]_n$,[10] and $[HgI_2((HOCH_2CH_2)_2dmit)]$.[11] The polymeric structures encountered in these materials result in part from a combination of $\pi-\pi$ and S···S interactions between the sulfur rich ligands, therefore these latters appear also as excellent candidates to promote intermolecular Au···Au interactions.

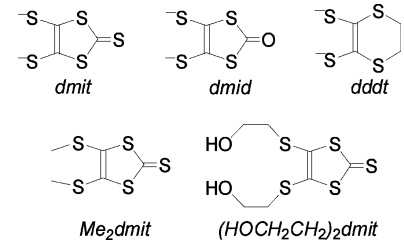

Experimental Section

Materials. $[AuCl(PPh_3)]$,[12] [AuCl(tht)],[13] *Me_2dmit*,[14] and *$(HOCH_2CH_2)_2$dmit*[15] were prepared according to the literature procedures. All manipulations were performed using Schlenk techniques in an atmosphere of dry oxygen-free argon.

Synthesis of $[Au_2(\mu$-dmid$)(PPh_3)_2]$ (1). A solution of 1,3,4,6-tetrathiapentalene-2,5-dione[16] (0.047 g; 0.225 mmol) in MeOH was reacted with a solution of MeONa (0.45 mmol). After stirring for 1 h, solid $[AuCl(PPh_3)]$ (0.223 g; 0.45 mmol) was added. The precipitate, which immediately appeared, was collected by filtration, washed with MeOH, and dried to provide **1** as a yellow-green solid. (0.200 g, 81% yield). Anal. found: C, 42.18; H, 2.80. $C_{39}H_{30}Au_2OP_2S_4$ calcd: C, 42.63; H, 2.75%. $^{31}P\{^1H\}$ NMR ($CDCl_3$): δ = 37.0; ^{13}C NMR ($CDCl_3$): δ = 193.5 (C═O); IR (KBr) ·/cm^{-1}: 1663 and 1613 (C═O). UV−vis (CH_2Cl_2) λ_{abs} (nm) (ϵ, $M^{-1}cm^{-1}$): 231 (43200), 303 (7500).

Synthesis of $[Au_2(\mu$-dddt$)(PPh_3)_2]$ (2). A solution of 5,6 dihydro-1,3dithiolo[4,5-b]-1,4-dithiine-2-one[17] (0.049 g; 0.235 mmol) in MeOH was reacted with a solution of MeONa (0.47 mmol). After stirring for 1 h, solid $[AuCl(PPh_3)]$ (0.232 g; 0.47 mmol) was added. The precipitate, which immediately appeared, was collected by filtration, washed with MeOH, and dried to provide **2** as a green solid. (0.215 g; 83% yield). Anal. found: C, 43.52; H, 3.09. $C_{40}H_{34}Au_2P_2S_4$ Calcd: C, 43.72; H, 3.12%. $^{31}P\{^1H\}$ NMR ($CDCl_3$): δ = 35.1. UV−vis (CH_2Cl_2) λ_{abs} (nm) (ϵ, $M^{-1}cm^{-1}$): 236 (36 800), 327 (7200).

(1) (a) King, C.; Wang, J. C.; Khan, M. N. I.; Fackler, J. P. *Inorg. Chem.* **1989**, *28*, 2145. (b) Yam, V. W.-W.; Lo, K. K. W. *Chem. Soc. Rev.* **1999**, *28*, 323. (c) Puddephatt, R. J. *Coord. Chem. Rev.* **2001**, *216−217*, 313. (d) Lagunas, M. C.; Mendicute Fiero, C.; Pintado-Alba, A.; de la Riva, H.; Betanzos-Lara, S. *Gold Bull.* **2007**, *40*, 135.

(2) (a) Assefa, Z.; McBurnett, B. G.; Staples, R. J.; Fackler, J. P., Jr.; Assmann, B.; Angermaier, K.; Schmidbaur, H. *Inorg. Chem.* **1995**, *34*, 75. (b) Forward, J. M.; Bohmann, D.; Fackler, J. P., Jr.; Staples, R. J. *Inorg. Chem.* **1995**, *34*, 6330. (c) Pintaldo-Alba, A.; de la Riva, H.; Nieuwhuyzen, M.; Bautista, D.; Raithby, P. R.; Sparkes, H. A.; Teat, S. J.; Lopez-de-Luzuriaga, J. M.; Lagunas, M. C. *J. Chem. Soc., Dalton Trans.* **2004**, 3459. (d) Tzeng, B. C.; Chan, C. K.; Cheung, K. K.; Che, C. M.; Peng, S. M. *J. Chem. Soc., Chem. Comm.* **1997**, 135. (e) de la Riva, H.; Pintado-Alba, A.; Nieuwenhuyzen, M.; Hardacre, C.; Lagunas, M. C. *J. Chem. Soc., Chem. Comm.* **2005**, 4970.

(3) (a) Yam, V. W.-W.; Li, C.-K.; Chan, C. L. *Angew. Chem., Int. Ed. Engl.* **1998**, *37*, 2857. (b) Yam, V. W.-W.; Chan, C. L.; Li, C.-K.; Wong, K. M.-C. *Coord. Chem. Rev.* **2001**, *216−217*, 173.

(4) (a) Davilla, R. M.; Elduque, A.; Grant, T.; Staplesand, R. J.; Fackler, J. P., Jr. *Inorg. Chem.* **1993**, *32*, 1749. (b) Gimeno, M. C.; Jones, P. G.; Laguna, A.; Laguna, M.; Terroba, R. *Inorg. Chem.* **1994**, *33*, 3932.

(5) (a) Pullen, A. E.; Olk, R. M. *Coord. Chem. Rev.* **1999**, *188*, 211. (b) Cassoux, P.; Valade, L.; Kobayashi, H.; Kobayashi, A.; Clark, R. A.; Underhill, A. E. *Coord. Chem. Rev.* **1991**, *110*, 115.

(6) (a) Cerrada, E.; Jones, P. G.; Laguna, A.; Laguna, M. *Inorg. Chem.* **1996**, *35*, 2995. (b) Cerrada, E.; Jones, P. G.; Laguna, A.; Laguna, M. *Inorg. Chim. Acta* **1996**, *249*, 163. (c) Cerrada, E.; Fernandez, E. J.; Jones, P. G.; Laguna, A.; Laguna, M.; Terroba, R. *Organometallics* **1995**, *14*, 5537.

(7) (a) Ryowa, T.; Nakano, M.; Tamura, H.; Matsubayashi, G. *Inorg. Chim. Acta* **2004**, *357*, 3532. (b) Cerrada, E.; Laguna, M.; Sorolla, P. A. *Polyhedron* **1998**, *17*, 295.

(8) (a) Guyon, F.; Lenoir, C.; Fourmigué, M.; Larsen, J.; Amaudrut, J. *Bull. Soc. Chim. Fr.* **1994**, *465*, 187. (b) Guyon, F.; Fourmigué, M.; Clérac, R.; Amaudrut, J. *J. Chem. Soc., Dalton Trans.* **1996**, 4093. (c) Jourdain, I.; Fourmigué, M.; Guyon, F.; Amaudrut, J. *Organometallics* **1999**, *18*, 1834. (d) Guyon, F.; Jourdain, I.; Knorr, M.; Lucas, D.; Monzon, T.; Mugnier, Y.; Avarvari, N.; Fourmigué, M. *Eur. J. Inorg. Chem.* **2002**, 2026. (e) Guyon, F.; Lucas, D.; Jourdain, I.; Fourmigué, M.; Mugnier, Y.; Cattey, H. *Organometallics* **2001**, *20*, 2421.

(9) Hameau, A.; Guyon, F.; Knorr, M.; Enescu, M.; Strohmann, C. *Monatsh. Chem.* **2006**, *137*, 545.

(10) (a) Dai, J.; Yang, W.; Ren, Z.-G.; Zhu, Q.-Y.; Jia, D.-X. *Polyhedron* **2004**, *23*, 1447. (b) Hameau, A.; Guyon, F.; Knorr, M.; Khatyr, A.; Strohmann, C. Manuscript in preparation.

(11) Ndiaye, A. L.; Guyon, F.; Knorr, M.; Huch, V.; Veith, M. *Z. Anorg. Allg. Chem.* **2007**, *633*, 1959.

(12) Uson, R.; Laguna, A. *Organomet. Synth.* **1985**, *3*, 325.

(13) Uson, R.; Laguna, A.; Laguna, M. *Inorg. Synth.* **1989**, *26*, 85.

(14) Steimecke, G.; Sieler, H. J.; Kirmse, R.; Hoyer, E. *Phosphorus Sulfur* **1979**, *7*, 49.

(15) Hansen, T. K.; Jorgensen, T.; Jensen, F.; Thygesen, P. H.; Christiansen, K.; Hursthouse, M. B.; Harman, M. E.; Malik, M. A.; Girmay, B.; Underhill, A. E.; Begtrup, M.; Kilburn, J. D.; Belmore, K.; Roepstorff, P.; Becher, J. *J. Org. Chem.* **1993**, *58*, 1359.

(16) Schumaker, R. R.; Lee, V. Y.; Engler, E. M. *J. Org. Chem.* **1984**, *49*, 564.

(17) Larsen, J.; Lenoir, C. *Synthesis* **1989**, 134.

Synthesis of [AuCl(Me$_2$dmit)] (3). To a solution of *Me$_2$dmit* (0.120 g; 0.5 mmol) in 10 mL of CH_2Cl_2 was added 1 equiv of [AuCl*(tht)*] (0.170 g; 0.5 mmol). The mixture was stirred at room temperature for 18 h. The yellow precipitate was then filtered and crystallized in hot $CHCl_3$. Yellow needles were obtained by cooling a $CHCl_3$ solution at −20 °C (0.200 g; 82% yield). Anal. found: C, 13.36; H, 1.46. $C_5H_6AuClS_5$ Calcd: C, 13.09; H, 1.32%. IR (KBr) ν/cm^{-1}: 1015 (C═S). UV−vis (CH_2Cl_2) λ_{abs} (nm) (ϵ, M^{-1}cm^{-1}): 243 (15300), 295 (6400), 433 (17 200).

Synthesis of [AuCl{(HOCH$_2$CH$_2$)$_2$dmit}] (4). To a solution of 4,5-bis[(2′-hydroxyethyl)thio]1,3-dithiole-2-thione (0.100 g; 0.349 mmol) in acetone (8 mL) was added 1 equiv of [AuCl*(tht)*] (0.112 g; 0.349 mmol) dissolved in acetone (7 mL). The resulting clear yellow-orange solution was stirred during 1 h at room temperature. After filtration, the filtrate was reduced to ca. 7 mL and cooled to allow formation of yellow crystals (0.105 g; 58% yield) suitable for X-ray measurement. Anal. found: C, 16.15; H, 1.84. $C_{14}H_{20}S_{10}O_4Au_2Cl_2$ Calcd: C, 16.20; H, 1.92%. ATR-IR ν/cm^{-1}: 3252 (OH), 1008 (C═S). ^{1}H NMR (DMSO-d_6): δ = 3.12 (4H, t, J = 6.2 Hz); 3.63 (4H, t, J = 6.2 Hz); 5.12 (2H, s, OH).

Apparatus. IR spectra have been recorded on a Nicolet Nexus 470 spectrometer. Elemental C, H analyses were performed on a Leco Elemental Analyzer CHN 900. The ^{31}P{^{1}H} NMR spectra were recorded at 300.13 MHz on a Bruker DRX 300 spectrometer. The chemical shifts are in ppm. The UV−vis spectra were recorded on a Uvikon-XL spectrometer and on a Hewlett-Packard diode array model 8452A. The emission and excitation spectra were obtained using a double monochromator Fluorolog 2 instrument from Spex. Phosphorescence time-resolved measurements were performed on a PTI LS-100 using a 1 μs tungsten flash lamp. Fluorescence and phosphorescence lifetimes were measured on a Timemaster Model TM-3/2003 apparatus from PTI. The source was nitrogen laser with high-resolution dye laser (fwhm ∼1300 ps) and the fluorescence lifetimes were obtained from high quality decays and deconvolution or distribution lifetimes analysis. The uncertainties were about ± 40 ps based on multiple measurements.

Quantum Yield Measurements. For room temperature, all samples were prepared under inert atmosphere (in a glovebox, P_{O2} < 20 ppm) by dissolution of the different compounds in 2-MeTHF using 1 mL quartz cells with septum (298 K) or quartz NMR tubes in liquid nitrogen for 77 K measurements. Two different measurements (i.e., different solutions) were performed for each photophysical data (quantum yields and Φ). The sample concentrations were chosen to correspond to an absorbance of 0.05 at the excitation wavelength. Each absorbance value was measured five times for better accuracy in the measurements of Φ_e. The reference for Φ_e was 9,10-diphenylanthracene (Φ_F = 1.0).[18]

Theoretical Computations. Calculations using the density functional theory (DFT) approximation were performed using the commercially available *Gaussian 03* software.[19] The hybrid B3LYP exchange-correlation function has been considered due to the high accuracy of the ensued results,[20–22] with the 3−21G* as the basis set for P, 6−31G(d) for carbon, hydrogen, and sulfur and LANL2DZ for gold.[23] All computations were performed without symmetry constraint.

Crystal-Structure Determinations. A suitable crystal of each complex was mounted in an inert oil (perfluoropolyalkylether) and used for X-ray crystal structure determinations. Data were collected on a Stoe IPDS diffractometer at 173(2) K for **1** and **2** and at 293 K for **4**. The intensities were determined and corrected by the program *INTEGRATE* in IPDS (Stoe & Cie, 1999). An empirical absorption correction was employed using the FACEIT-program in IPDS (Stoe & Cie, 1999). All structures were solved applying direct and Fourier methods, using *SHELXS-90* and *SHELXL-97*.[24,25] For each structure, the non-hydrogen atoms were refined anisotropically. All of the hydrogen atoms were placed in geometrically calculated positions and each was assigned a fixed isotropic displacement parameter based on a riding-model. Refinement of the structures was carried out by full-matrix least-squares methods based on F_o^2 using *SHELXL-97*. All calculations were performed using the *WinGX* crystallographic software package, using the programs *SHELXS-90* and *SHELXL-97*. The crystallographic data for each complex are given in Table 1.

Results and Discussion

Synthesis of 1,2-Dithiolene Bridged Dinuclear Gold(I) Complexes. The preparation of [{Au(PPh$_3$)}$_2$(*μ-dmid*)] (**1**) and [{Au(PPh$_3$)}$_2$(*μ-dddt*)] (**2**) was performed by the reaction of the dithiolene dianion with 2 equiv of [AuCl(PPh$_3$)]. The ligands *dmid* and *dddt* are obtained from the corresponding 1,3-dithiol-2-ones by treatment with sodium methanolate (Scheme 1). The dinuclear **1** and **2** complexes are obtained as green-yellow crystalline solids and are air-stable.

The ^{31}P{^{1}H} NMR spectra of both compounds exhibit a broadened singlet at room temperature, indicating the presence of two magnetically equivalent phosphorus atoms in solution. At 296 K, the proton NMR spectrum of the ethylenic segment of **2** consists in a AA′BB′ pattern centered at 3.27 ppm. This is indicative of a nonequivalence of the two faces of the dithiolene core. The fluxional behavior in solution of a similar system has been studied elsewhere by means of temperature-dependent NMR spectroscopy.[8b]

Structural Analysis of 1 and 2. Suitable single crystals of **1** and **2** were grown from CH_2Cl_2/hexane. **1** crystallizes with one solvent molecule of CH_2Cl_2. Their molecular structures shown in Figures 1 and 2 are very reminiscent to those of the structurally characterized [{Au(PR$_3$)}$_2$(*μ-dithiolene*)] complexes. Selected bond lengths and angles are listed in Table 2 and were compared with those of [{Au-

(18) Morris, J. V.; Mahaneyand, M. A.; Huber, J. R. *J. Phys. Chem.* **1976**, *80*, 969.

(19) Frisch, M. J.; Trucks, G. W.; Schlegel, H. B.; Scuseria, G. E.; Robb, M. A.; Cheeseman, J. R.; Montgomery, J. A.; Vreven, J. T.; Kudin, K. N.; Burant, J. C.; Millam, J. M.; Iyengar, S. S.; Tomasi, J.; Barone, V.; Mennucci, B.; Cossi, M.; Scalmani, G.; Rega, N.; Petersson, G. A.; Nakatsuji, H.; Hada, M.; Ehara, M.; Toyota, K.; Fukuda, R.; Hasegawa, J.; Ishida, M.; Nakajima, T.; Honda, Y.; Kitao, O.; Nakai, H.; Klene, M.; Li, X.; Knox, J. E.; Hratchian, H. P.; Cross, J. B.; Adamo, C.; Jaramillo, J.; Gomperts, R.; Stratmann, R. E.; Yazyev, O.; Austin, A. J.; Cammi, R.; Pomelli, C.; Ochterski, J. W.; Ayala, P. Y.; Morokuma, K.; Voth, G. A.; Salvador, P.; Dannenberg, J. J.; Zakrzewski, V. G.; Dapprich, S.; Daniels, A. D.; Strain, M. C.; Farkas, O.; Malick, D. K.; Rabuck, A. D.; Raghavachari, K.; Foresman, J. B.; Ortiz, J. V.; Cui, Q.; Baboul, A. G.; Clifford, S.; Cioslowski, J.; Stefanov, B. B.; Liu, G.; Liashenko, A.; Piskorz, P.; Komaromi, I.; Martin, R. L.; Fox, D. J.; Keith, T.; Al-Laham, M. A.; Peng, C. Y.; Nanayakkara, A.; Challacombe, M.; Gill, P. M. W.; Johnson, B.; Chen, W.; Wong, M. W.; Gonzalez, C.; Pople, J. A. *Gaussian 03*, RC, Ed.; Gaussian, Inc.: Wallingford, CT, 2004.

(20) Becke, A. D. *J. Chem. Phys.* **1993**, *98*, 5648.

(21) Lee, C.; Yang, W.; Parr, R. G. *Phys. Rev. B, Condens. Matter* **1988**, *37*, 785.

(22) Miehlich, B.; Savin, A.; Stoll, H.; Preuss, H. *Chem. Phys. Lett.* **1989**, *157*, 200.

(23) (a) Dobbs, K. D.; Hehre, W. J. *J. Comput. Chem.* **1986**, *7*, 359. (b) Dobbs, K. D.; Hehre, W. J. *J. Comput. Chem.* **1987**, *8*, 861. (c) Dobbs, K. D.; Hehre, W. J. *J. Comput. Chem.* **1987**, *8*, 880.

(24) G. M. Sheldrick *SHELXS-90*; University of Göttingen: Göttingen, Germany, 1990.

Table 1. Crystallographic data for **1**, **2**, and **4**

identification code	**1·CH_2Cl_2**	**2**	**4**
empirical formula	$C_{40}H_{32}Au_2Cl_2OP_2S_4$	$C_{40}H_{34}Au_2P_2S_4$	$C_{14}H_{20}Au_2Cl_2O_4S_{10}$
fw	1183.67	1098.79	1037.73
wavelength	0.71073 Å	0.71073 Å	0.71073 Å
cryst syst	monoclinic	monoclinic	monoclinic
space group	*P*2(1)/*n*	*P*2(1)	*P*2(1)/*n*
unit cell dimensions	a = 10.928(2) Å, b = 10.726(2) Å, c = 34.297(7) Å, β = 95.18(3)°	a = 10.528(2) Å, b = 10.691(2) Å, c = 16.689(3) Å, β = 98.94(3)°	a = 5.4398(11) Å α= 90°. b = 30.511(6) Å β= 105.49(3)°. c = 8.6704(17) Å β = 105.49(3)°
V	4003.6(14) Å^3	1855.7(6) Å^3	1386.8 (5) Å^3
Z	4	2	2
D_{calcd}	1.964 mg/m^3	1.996 mg/m^3	2.485 mg/m^3
absorption coefficient	7.775 mm^{-1}	8.237 mm^{-1}	11.535 mm^{-1}
F(000)	2264	1052	976
cryst size	0.30 × 0.20 × 0.20 mm^3	? × ? × ? mm^3	0.7 × 0.1 × 0.05 mm^3
θ range for data collection	2.24 to 26.00°	2.15 to 27.00°	2.53 to 27.98°
index ranges	$-13 \le h \le 13$, $-13 \le k \le 13$, $-42 \le l \le 42$	$-13 \le h \le 13$, $-13 \le k \le 13$, $-21 \le l \le 21$	$-6 \le h \le 6$, $-40 \le k \le 39$, $-11 \le l \le 11$
reflns collected	7829	15925	12410
independent reflns	6429 [R(int) = 0.0591]	8019 [R(int) = 0.0505]	3107 [R(int) = 0.0798]
refinement method	Full-matrix least squares on F^2	Full-matrix least squares on F^2	Full-matrix least squares on F^2
data/restraints/params	7828/0/460	8019/1/433	3107/0/148
GOF on F^2	1.061	1.010	1.034
final R indices [$I > 2\sigma(I)$]	R1 = 0.0368, wR2 = 0.0923	R1 = 0.0442, wR2 = 0.1092	R1 = 0.0270, wR2 = 0.0629
R indices (all data)	R1 = 0.0461, wR2 = 0.0959	R1 = 0.0492, wR2 = 0.1143	R1 = 0.0396 wR2 = 0.0674
largest diff. peak and hole	1.392 and −1.141 e·Å^{-3}	1.625 and −2.012 e·Å^{-3}	1.074 and −1.219 e·Å^{-3}

Scheme 1. (i) 2 equiv NaOMe in MeOH, (ii) 2 equiv [AuCl(PPh_3)$_2$]

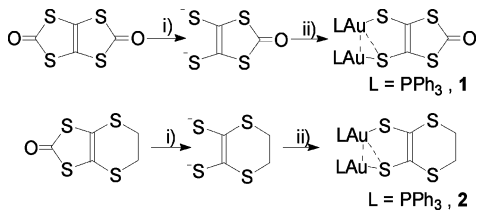

(PPh_3)}$_2$(μ-*dmit*)][6a] and [{Au(PPh_3)}$_2$(μ-*mnt*)] (*mnt* = 1,2-dicyanoethene-1,2-dithiolate).[4a] In **1** and **2**, the two gold atoms are bridged by the 1,2-dithiolene, and each one is coordinated to a PPh_3 with typical Au−S and Au−P distances (in the range 2.311(2)−2.344(2) and 2.254(2)−2.274(2) Å, respectively). The geometry about one gold atom is approximately linear (S(2)−Au(2)−P(2) = 172.47(5)° for **1** and 173.41(9)° for **2**), but the coordination of the second

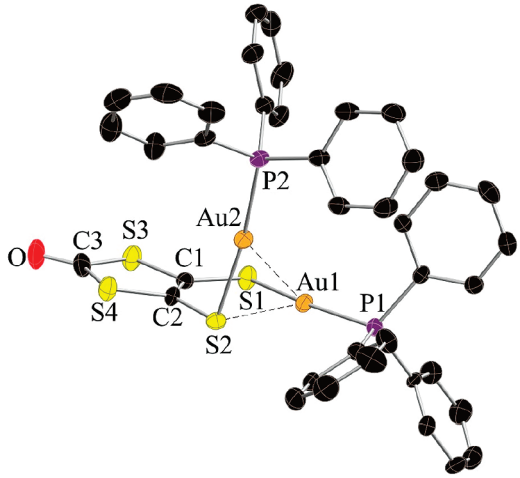

Figure 1. Thermal ellipsoid plot of **1** (50% level). Hydrogen atoms and solvated CH_2Cl_2 are omitted for clarity.

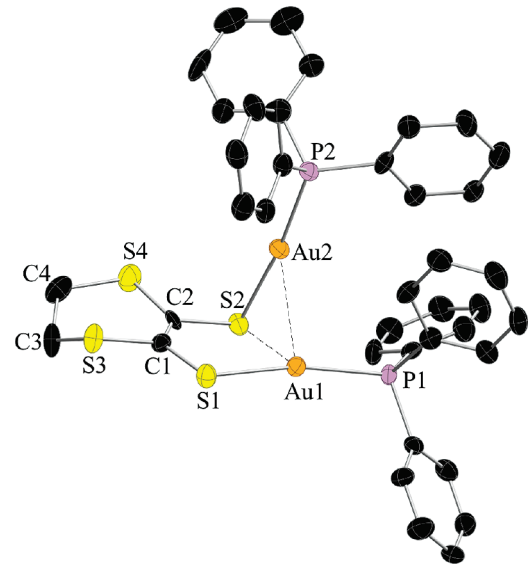

Figure 2. Thermal ellipsoid plot of **2** (50% level). Hydrogen atoms are omitted for clarity.

gold deviates more significantly from linearity [S(1)−Au(1)−P(1) = 165.16(5)° for **1** and 163.40(8)° for **2**] due to the existence of an additional Au···S interaction [Au(1)−S(2) = 2.720(2) Å for **1** and 2.830(2) Å for **2**]. This unsymmetrical coordination around the gold(I) centers is a common feature for the 1,2-dithiolene ligands. Fackler et al. have shown that electronic rather than steric factors are responsible for the irregular geometries observed.[26] Only one of the atoms of gold is almost coplanar to the 1,3-dithiole-2-thione skeleton. Both complexes exhibit Au···Au intramolecular

(25) G. M. Sheldrick *SHELXL-97*; University of Göttingen: Göttingen, Germany, 1997.
(26) Davila, R. M.; Staples, R. J.; Elduque, A.; Harlass, M. M.; Kyle, L.; Fackler, J. P., Jr. *Inorg. Chem.* **1994**, *33*, 5940.

Table 2. Selected Bonds (Angstroms) and Angles (Degrees) of [(AuL)$_2$(μ-dithiolene)] (L = PPh$_3$)

	1	**2**	[(AuL)$_2$ (μ-dmit)][6a]	[(AuL)$_2$ (μ-mnt)][4a]
Au(1)−S(1)	2.3441(17)	2.321(2)	2.3435(12)	2.323(4)
Au(2)−S(2)	2.3366(15)	2.311(2)	2.3474(11)	2.321(4)
Au(1)−S(2)	2.7203(16)	2.830(2)	2.8226(14)	2.811(5)
Au(1)−Au(2)	3.1985(10)	3.1295(11)	3.0681(8)	3.115(3)
Au(1)−P(1)	2.2709(16)	2.274(2)	2.2569(12)	2.273(4)
Au(2)−P(2)	2.2652(15)	2.254(2)	2.2779(11)	2.269(4)
C(1)−S(1)	1.761(6)	1.747(9)	1.740(4)	1.729(18)
C(2)−S(2)	1.761(7)	1.769(10)	1.749(4)	1.751(15)
C(1)−C(2)	1.340(9)	1.349(14)	1.362(5)	1.372(24)
S(1)−Au(1)−P(1)	165.16(5)	163.40(8)	159.32(4)	158.9(2)
S(2)−Au(2)−P(2)	172.47(5)	173.41(9)	174.86(3)	174.7(1)
S(1)−Au(1)−Au(2)	95.30(4)	96.34(6)	92.54(3)	
P(1)−Au(1)−Au(2)	97.26(4)	98.57(6)	103.10(3)	
Au(1)−S(1)−C(1)	102.6(2)	107.8(3)	104.15(14)	106.4(5)
Au(2)−S(2)−C(2)	96.0(2)	97.4(3)	102.39(13)	103.9(5)

Scheme 2. (i) Toluene reflux for 15 h

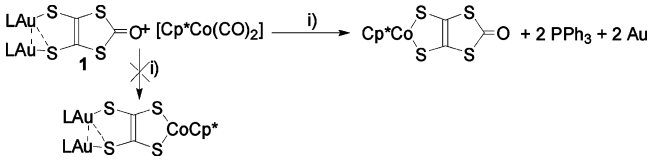

interactions. The Au(1)−Au(2) distance of **1** [3.1984(10) Å] is longer than the one of **2** [3.1295(11) Å], which is typical of this type of complex. No S···S short contacts are noted in the solid state.

Recently, we reported on a novel efficient method for the preparation of dimetallic cyclopentadienyl cobalt complexes bridged by the ethylenetetrathiolate $C_2S_4^{4-}$ ligand.[8d] The reaction consists of the oxidative addition of 1,3-dithiol-2-one across [Cp*Co(CO)$_2$] (Cp* = η^5-C$_5$Me$_5$). With the aim to obtain the first heterodimetallic complex bridged by the ethylenetetrathiolate ligand, we react **1** with 1 equiv of [Cp*Co(CO)$_2$] in refluxing toluene. Unfortunately, all attempts to isolate the desired product were unsuccessful. Instead, we observed the deposition of a gold mirror inside the Schlenk tube together with the formation of diamagnetic [Cp*Co(*dmid*)] (Scheme 2), which was identified by its intense deep-green color and comparison of its NMR spectrum.[8d] In summary, the [Co^I] fragment reduces the gold(I) atoms rather than the 1,3-dithiol-2-one function.

Synthesis of [AuCl(Me$_2$dmit)] (3) and [AuCl{(HOCH$_2$CH$_2$)$_2$dmit}] (4). The commonly used gold precursor [AuCl(tht)] (tht = tetrahydrothiophene) is known for the lability of the sulfide ligand, facilitating its substitution by other neutral or anionic ligands.[13] Thus, *Me$_2$dmit* and *(HOCH$_2$CH$_2$)$_2$dmit* react with [AuCl(tht)] in a 1:1 metal-to-ligand ratio at room temperature to afford yellow crystals of [AuCl(*Me$_2$dmit*)] (**3**) and [AuCl{*(HOCH$_2$CH$_2$)$_2$dmit*}] (**4**) in 82% and 58% yield, respectively. The compositions of the air stable isolated products were established by elemental analysis and single crystal X-ray diffraction studies (below). The UV−vis absorption spectra of **3** and the *Me$_2$dmit* ligand measured in CH_2Cl_2 at room temperature are dominated by an intraligand charge transfer ($\pi \rightarrow \pi^*$) between 230 and 340 nm centered on the C=C and C=S groups (Supporting Information). Upon coordination, the lowest energy band of

Scheme 3

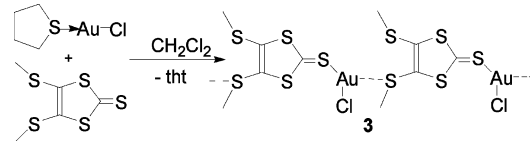

the ligand at 394 nm is shifted toward lower energy to appear at 433 nm in **3**. With reference to earlier spectroscopic studies of gold thione complexes,[27] this lowest energy band can be assigned to electronic transition from a sulfur *n* lone pair to the (C=S) π^* orbital ($n \rightarrow \pi^*$). Although the poor quality of the crystals of **3** does not allow a detailed discussion of the crystal structure,[28] the coordination mode of *Me$_2$dmit* on [AuCl] fragment could be described as outlined in Scheme 3. The complexation on gold occurs via the thiocarbonyl function as observed in the case of CuI and HgX_2 adducts.[9,10] Both the length of the Au−S bond of about 2.213 Å and the Cl−Au−S bond angle of 174.2° lie in a similar range found for thione **4** (below). An additional weak contact of 3.21 Å is also identified between a thioether function and a second AuCl fragment. By this manner, *Me$_2$dmit* acts as a bridging ligand between AuCl fragments, leading to the formation of a 1D coordination polymer (Scheme 3). The coordination mode via the sulfur of the thioketone group is also confirmed by the IR spectra because the C=S vibration appears at lower position in **3** than in the free ligand (1015 vs 1057 cm^{-1}). A comparable shift to lower wavenumbers is also observed for the C=S vibration measured in **4** (1008 cm^{-1}) and that recorded for *(HOCH$_2$CH$_2$)$_2$dmit* (1070 cm^{-1}). Furthermore, the ATR-IR spectrum of **4** indicates the presence of hydrogen bonds because broad OH vibrations were observed at 3252 cm^{-1}.

Structural analysis of 4. Compared to **3**, complex **4** displays a very different architecture, which consists of a dimeric structural motif. It results from a surprisingly close aurophilic contact of 3.078(6) Å between the two metal centers as depicted in Figure 3. A similar arrangement in antiparallel pairs was reported for the thione complex [AuCl(C$_3$H$_4$S$_3$)] (C$_3$H$_4$S$_3$ = ethylenthiocarbonate) with a Au···Au separation of 3.366 Å.[27] More recently, an Au···Au contact of 3.1488(7) Å was established in the dimeric association of two gold(I) macrocycles.[29] The intermolecular Au···Au distance in **4** is also significantly shorter than the intramolecular semi-supported interactions observed for **1** and **2** (Table 2), in which the two gold atoms are held in close proximity by the clamping effect of the two bridging ligands. The close contact in **4** may better be compared with the distances of 3.023(1) and 3.0038(6) Å reported for semi-supported [ClAu(μ-dppdiene)AuCl] (dppdiene = 2,3-(bisphenylphosphino)-1,3-butadiene) and [ClAu(μ-dpephos)AuCl] (dpephos = bis(2-diphenylphosphino)phenylether), respectively.[30a,b] This value is not so

(27) Raubenheimer, H. G.; Otte, R.; Linford, L.; Van Zyl, W. E.; Lombard, A.; Kruger, G. J. *Polyhedron* **1992**, *11*, 893.
(28) Crystal data for **3** (at 293 K): monoclinic, $P2_1$, a = 7.3521, b = 9.4866, c = 8.0530 Å, β = 94.171°, V = 560.2(2) Å^3, Z = 2.
(29) (a) Mohr, F.; Jennings, M. C.; Puddephatt, R. J. *Eur. J. Inorg. Chem.* **2003**, 217.

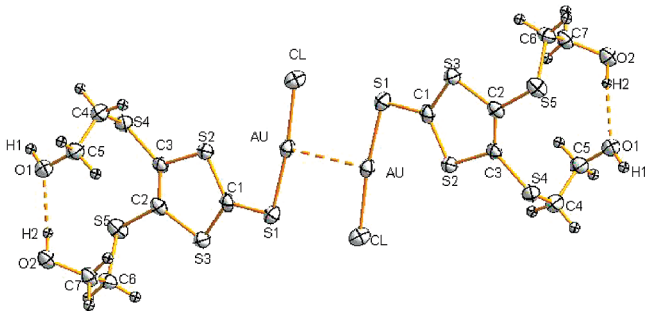

Figure 3. Thermal ellipsoid plot of **4** (50% level). Selected bond lengths (Å) and angles (°): Au−S(1) 2.293(2), Au−Cl 2.293 (2), Au−Au# 3.078(6), S(1)−C(1) 1.702(5), S(2)−C(1) 1.714(5), S(1)−C(1) 1.702(5), S(2)−C(1) 1.714(5), S(2)−C(3) 1.752(6), S(3)−C(1) 1.714(6), S(3)−C(2) 1.758(5), S(4)−C(3) 1.768(5), S(4)−C(4) 1.818(7), S(5)−C(2) 1.767(6), S(5)−C(6) 1.840(6), C(3)−C(2) 1.353(8), C(4)−C(5) 1.523(8), C(6)−C(7) 1.513(8), C(5)−O(1) 1.419(8), C(7)−O(2) 1.427(6), S(1)−Au−Cl 173.59(5), S(1)−Au−Au#1 102.27(4), Cl−Au−Au#1 84.00(4), C(1)−S(1)−Au 100.30(19), C(1)−S(2)−C(3) 96.7(3), C(1)−S(3)−C(2) 96.3(3), C(3)−S(4)−C(4) 100.4(3). # denotes symmetry related atoms.

different from those found for the fully supported dppm-spanned dinuclear complexes [ClAu(μ-dppm)$_2$AuCl] (2.96-(1) Å), [(Au(μ-dppm)$_2$Au][BF$_4$]$_2$ (2.931(1) Å), [(Au(μ-dppm)$_2$Au][PF$_6$]$_2$ (2.9792(10) Å), or the tetranuclear compound [(OC)$_3$Fe{Si(OMe)$_3$}(μ-dppm)Au]$_2$ (2.9622(1) Å).[30c−g] The 1,3-dithiole-2-thione-4,5-dithiolate skeleton and the AuCl fragment are almost coplanar. Due to the torsion angle Cl−Au−Au−Cl of 180°, the Au···Cl# and Cl#···S1 distances are quite short and amount to 3.641(7) and 3.326(5) Å, respectively. The hydroxyethyl side-chains adopt a *syn*-orientation relatively to this plane and allow the formation of intramolecular hydrogen bonds. The O(1)···O(2) separation in the resulting eleven-membered ring is similar to that determined recently by us for the free ligand (2.801(6) vs 2.790(3) Å).[11] The Cl−Au−S bond angle of 173.59° deviates slightly from linearity.

The C═S bond length of 1.702(5) Å is elongated with respect to that reported for ligand *(HOCH$_2$CH$_2$)$_2$dmit* (1.644(2) Å),[11] suggesting a strong coordination of this sulfur rich ligand to the gold(I) atom. The Au−S bond distance corroborates this observation because its value of 2.293(2) Å is similar to that reported in gold(I) thiolate complexes [Au(PPh$_3$)(SPh)] (2.30(1) and 2.32(1) Å)[31] and [Au(PPh$_3$)-{SPh(*o*-Cl)}] (2.292(2) Å).[2b] In contrast with the coordination polymer **3**, the thioether groups of **4** are not involved in any bonding interactions. In addition to the intramolecular hydrogen bonds, O(1) is connected to O(2) of an adjacent dimeric unit via intermolecular hydrogen bonds, thus generating a supramolecular network (Supporting Information). The O···O distance of the intermolecular interaction is similar to that of the intramolecular one (2.814(7) vs 2.801(6) Å). The intermolecular O−H···O angle is less deviated from linearity than the intramolecular one (177.70° vs 165.83°). Other literature-known gold compounds combining strong hydrogen bonding and aurophilic attraction exist. For example, the cooperative force of aurophilic and hydrogen bonding were recently used to self-assemble supramolecular networks, exploiting the propensity of thiobarbituric derivatives, which strongly interact both with both Au(I), to form NH···O and OH···H bonds.[32]

Electronic Structure and Photophysics. The X-ray structures of **1** and **2** reveal the presence of two nonequivalent Au(PPh$_3$) units due to their relative orientations with the π-system-containing electron rich residue dithiolene. Therefore, two possible chromophores (and lumophores) sites are available. In addition, close intramolecular Au···S and Au···Au contacts are also evident, thus creating the possibility of other low-lying excited states such Au···Au centered dσ*pσ. It is known from the literature that gold(I) thiolate complexes such as (Ph$_3$P)AuSPh and (Ph$_3$P)AuS(C$_6$H$_4$-*o*-OMe) exhibit room temperature luminescence at 413 and 429 nm when excited at 360 and 350 nm, with emission lifetimes (τ_e) of 17 and 75 μs, respectively.[2b] These emissions are assigned to a ligand-to-metal-charge-transfer (LMCT) from a thiolate residue to the gold center. The authors also clearly demonstrated the electronic behavior when Au···Au contacts are close enough to split the orbitals Au (6pz) and S(pπ), thus creating an intramolecular dσ*pσ excited-state that generates a red-shifted emission. On the basis of the crystallographic results, **1**, **2**, and **4** are good candidates to exhibit such excited states, and their emitting properties should also depend on the Au···Au interactions. To describe and assign the electronic transitions and MOs, DFT, and TDTFT calculations were performed. All of the spectroscopic and photophysical data are presented in Table 3.

Complex **1**. Using the X-ray data for **1**, the nature of the HSOMO (triplet-state highest singly occupied molecular orbital) and HOMO (singlet state highest occupied molecular orbital) are computed, as well as the energy difference, to address the nature of the observed long-lived emission. These two MOs involved in the transition are presented in Figure 4. The triplet state is primarily located onto the Au···Au units, whereas the HOMO is mainly composed of the dithiolene π system. The calculated emission wavelength is 436 nm for the crystal geometry at 173 K, comparing favorably to that experimentally found (410 nm at 298 K, Figure 5). This comparison is considered fair and we assign the emission to a LMCT excited state where M is the two interacting gold units and L is the dithiolene. These computations and conclusions agree with those of Forward et al.[2b] on a similar system.

(30) (a) Schmidbaur, H.; Dziwok, K.; Grohmann, A.; Müller, G. *Chem. Ber.* **1989**, *122*, 893. (b) de la Riva, H.; Pintado-Alba, A.; Nieuwenhuyzen, M.; Hardacre, C.; Lagunas, M. C. *Chem. Commun.* **2005**, 4970. (c) Schmidbaur, H.; Wohlleben, A.; Schubert, U.; Frank, A.; Huttner, G. *Chem. Ber.* **1977**, *110*, 2751. (d) The Au···Au separation of 3.351(2) Å in [ClAu(μ-dppm)AuCl] is considered as short, but nonbonding. Schmidbaur, H.; Wohlleben, A.; Wagner, F. E.; Orama, O.; Huttner, G. *Chem. Ber.* **1977**, *110*, 1748. (e) Porter, L. C.; Khan, Md. N. I.; King, C.; Fackler, J. P. *Acta Crystallogr.* **1989**, *C45*, 947. (f) Wu, M.; Zhang, L.; Chen, Z. *Acta Crystallogr.* **2003**, *E59*, m72. (g) Braunstein, P.; Knorr, M.; Tiripicchio, A.; Tiripicchio Camellini, M. *Inorg. Chem.* **1992**, *31*, 3685.

(31) Onaka, S.; Katsukawa, Y.; Shiotsuka, M.; Kanegawa, O.; Yamashita, M. *Inorg. Chim. Acta* **2001**, *312*, 100.

(32) (a) Hollatz, C.; Schier, A.; Schmidbaur, H. *J. Am. Chem. Soc.* **1997**, *119*, 8115. (b) Hunks, W. J.; Jennings, M. C.; Puddephatt, R. J. *Inorg. Chem.* **2002**, *41*, 4590. (c) Supramolecular structures may also result from the combination of aurophilic and $\pi-\pi$ interactions Nunokawa, K.; Okazaki, K.; Onaka, S.; Ito, M.; Sunahara, T.; Ozeki, T.; Imai, H.; Inoue, K. *J. Organomet. Chem.* **2005**, *690*, 1332.

Table 3. Spectroscopic and Photophysical Data of **1**, **2**, and **4**

compounds	λ_{abs} (nm) (ϵ, M^{-1} cm^{-1})[b]	λ_{em} (nm)	τ_e	Φ[b]
1	238 (45 100) 318 (6900)	400 and 550[a] 370[b] 450 and 685[c] 410[d]	phosphorescence (μs): 37 ± 5 at 450 nm[a] 250 ± 7 at 570 nm[a] 0.017 ± 0.002 at 400 nm[a] 78 ± 14 at 400 nm[c] 139 ± 20 at 650 nm[c] 70 ± 4 at 400 nm[d]	0.6%
2	241 (38 750) 327 (7800)	450 and 600[a] 380[b] 405 and 480[c] 405 and 480[d]	phosphorescence (μs): 72 ± 16 at 440 nm[a] 248 ± 10 at 600 nm[a] 2 at 320 nm[b] 95 ± 4 at 400 nm[c] 65 ± 20 at 400 nm[d]	0.5%
4	244 (18 800) 424 (12 750)	510 and 610[a] 670[c] 615[d]	fluorescence (ns): 1.38 ± 0.02 at 510 nm[a] phosphorescence (μs): 676 ± 13 at 580 nm[a] 191 ± 7 at 510 nm[a]	2.6%[e]

[a] In 2-MeTHF at 77 K. [b] In 2-MeTHF at 298 K. [c] In solid state at 77 K. [d] In solid state at 298 K. [e] Sum of Φ_F and Φ_P.

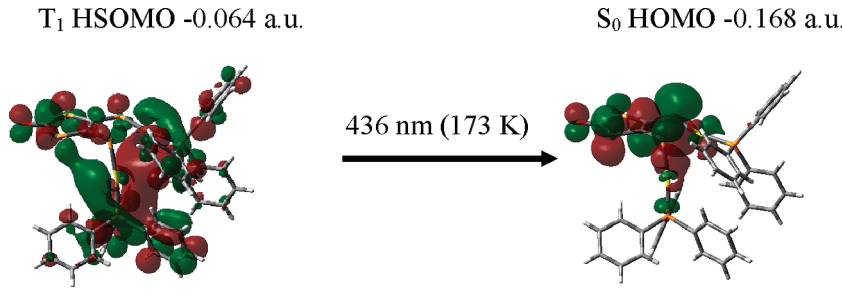

Figure 4. MO representations of the HOMO and HSOMO involved in the triplet emission for **1**. The calculated emission is found at 436 nm in the solid state at 173 K. The observed maxima are at 410 nm at 298 K and 685 nm at 77 K in the solid state.

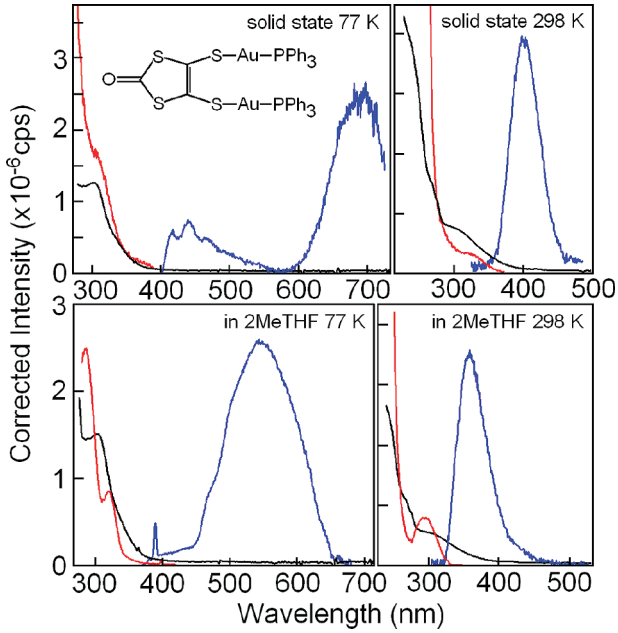

Figure 5. Emission (blue), excitation (red), and absorption spectra (black) of **1** in the solid state and in 2-MeTHF solution at 77 and 298 K. The absorption spectra indicated in the solid-state spectra are those of the solution for comparison purposes. The sharp peak at 395 nm is an artifact.

Upon cooling the samples, the close Au···Au contacts shorten because of the flexibility of the two dangling $AuPPh_3$ branches. The strengthening (i.e., shortening) of the Au···Au interactions induces a red-shift of the emission band. Indeed, the new emission maximum is now observed at 685 nm for the solid state at 77 K (Figure 5). Conversely, in solution at 298 K where there is no constraint to rotation about the C−S single bonds, the complex should adopt one or many flexible configurations (rotamers) where the intramolecular steric interactions between the $AuPPh_3$ fragments are minimized. As a consequence a blue-shifted emission is anticipated. Indeed, this band is observed at 370 nm (Figure 5). In such a case, the emission is also assigned to a LMCT, but the two gold units are not interacting and the assignment is an LMCT where M is a single metal center. A broadband centered at 550 nm for **1** in a 77 K frozen solution is also observed. It is believed that the broad envelope includes a series of emission bands arising from frozen different rotamers between the two extreme cases, close Au···Au contacts (685 nm), and open conformation (370 nm) described above.

TDDFT calculations were performed in an attempt to describe the absorption spectra. The results are difficult to interpret because no simple HOMO−LUMO transition is computed. Instead, the TDDFT computations indicate the presence of many small absorption transition vectors in the 321−342 nm window. The knowledge of the nature of the T_1 state can now be tentatively used as a landmark to find out what the most probable transition in the absorption may be. However, knowing that we must have an absorption band around 318 nm (Figure 5), and that the S_1 excited-state must be closely related to the T_1 excited state, the TDDFT computations indicate only the presence of a single logical candidate for a possible MO with a singlet transition

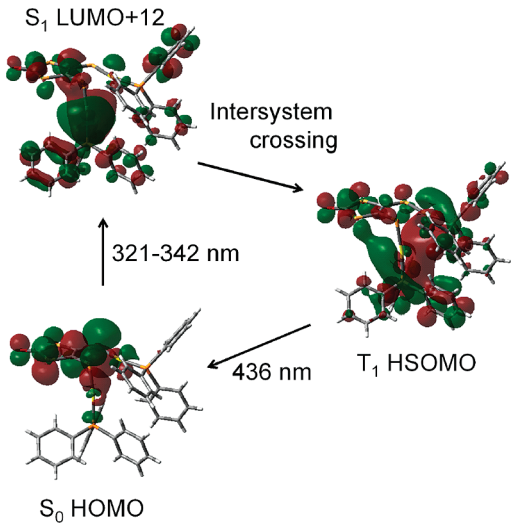

Figure 6. Calculated MOs for **1** for the MOs involved in the absorption and emission spectra.

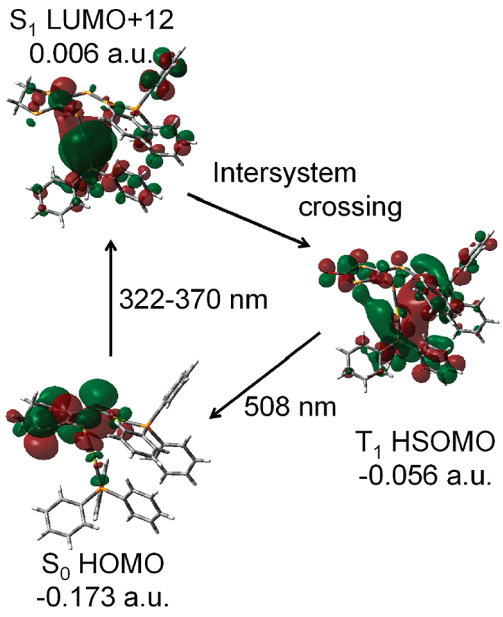

Figure 7. Calculated MOs for **2** for the MOs involved in the absorption and emission spectra.

in the 321 to 342 nm range. This MO is LUMO+12, which also exhibits the largest oscillator strength. It also bears close resemblance to HSOMO (Figure 6), and is the first empty gold-based orbital. It is located at 0.063 a.u. higher in energy than the HSOMO. All in all, the absorption spectrum is probably governed by an LMCT (where M is a single gold unit) as presented in Figure 6, and intersystem crossing populates a triplet state where the MOs include both gold metals.

Complex **2**. The crystal structure and luminescence properties are very similar to **1**, so the electronic spectra and computational results are found unsurprisingly similar. The HOMO and HSOMO (triplet) are computed by DFT using the X-ray structure data for **2** as well as TDDFT is used for assignment purposes. The same conclusions are drawn below (Figure 7).

The emission spectra of **2** at 298 K in the solid exhibit a structured emission on the low-energy side of the spectra at

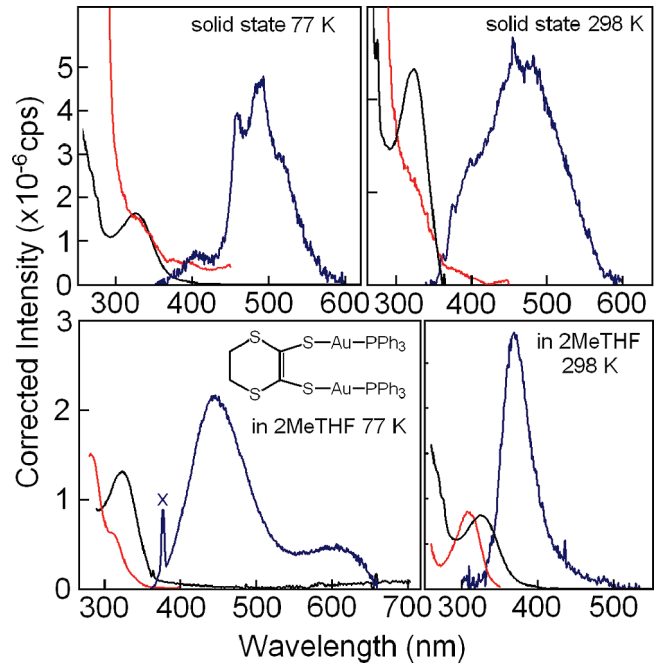

Figure 8. Emission (blue), excitation (red), and absorption spectra (black) of **2** in the solid state and in 2-MeTHF solution at 77 and 298 K. The absorption spectra indicated in the solid-state spectra are those of the solution for comparison purposes. The sharp peak (*x*) at 395 nm is an artifact.

~480 nm (Figure 8). On the basis of the TDDFT computations, which place this emission at 508 nm (Figure 7), the assignment for this phosphorescence is the same (i.e., LMCT where M is the two Au units and L is still the electron rich dithiolene).

However, on the high-energy side of the solid-state spectra at 77 and 298 K, a structureless emission centered at 405 nm is observed. This emission exhibits an excitation spectrum that matches the absorption (in solution) and reminds that found in **1** in the same range. We would like to propose that this emission is also LMCT but for a rotamer where the Au···Au interactions are not as pronounced as the former. In other words, the powder is not homogeneous, whereas crystals for structure determination were obtained only for one of them. This proposal is supported by the observation of one and two emission bands for **2** in 2-MeTHF at 298 and 77 K, respectively (Figure 8). At 298 K, the 370 nm band is associated with a rotamer, where the intramolecular Au···Au interactions are minimal for steric reasons. As the temperature is decreased to 77 K, two bands are depicted at ~450 and ~600 nm. These trapped species exhibit different emission lifetimes as demonstrated by time-resolved spectroscopy (Figure 9). These two species do not exhibit the same lifetime. These are assigned to two different conformers depending on the relative amplitude of Au···Au interactions.

The TDDFT computation analysis applied for the absorption spectra are also very similar to **1**, giving a predicted LMCT absorption around 322−370 nm based on the multiple possible calculated lower-energy transitions. Again, the electronic transition HOMO to LUMO +12, the first MO based on the gold centers, exhibits the largest computed oscillator strength. Experimentally, a band at 327 nm is observed in solution.

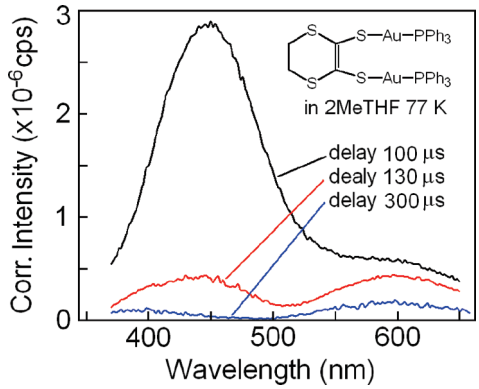

Figure 9. Time-resolved emission (low-resolution) spectra of **2** in 2-MeTHF at 77 K, demonstrating evidence for two emitting species.

In summary, the solid-state spectra of structurally quite similar **1** and **2** exhibit at 298 K emission maxima at ~410 and ~480 nm, respectively. These results are consistent with the shorter Au···Au separation in **2** (3.20 Å for **1** and 3.13 Å for **2**). In solution at 298 K, the emission maxima are closer (370 nm for **1** and 380 nm for **2**), which is consistent with free rotations about the C−S bond that may lead to conformation where no Au···Au interaction exists or is very weak. So, the emission arises from a LMCT excited-state involving a noninteracting $SAuPPh_3$. At 77 K, the solid-state spectra exhibit emission maxima at ~685 and ~480 nm for **1** and **2**, respectively. These LMCT emissions are obviously different. The explanation stems from the different crystal systems (above). Upon cooling, the contraction of the unit-cell dimensions may be different. Unfortunately, we do not have the X-ray structures of these compounds at 77 K to confirm this hypothesis.

Complex **4**. This case turns out to be much simpler than that for **1** and **2**. The emission spectra of **4** are presented in Figure 10. The spectra are characterized by an emission band centered at ~615 nm at 298 K, which is red-shifted at 77 K to 670 nm. Again, DFT and TDDFT computations are used to assign the electronic spectra. For the interpretation of the solid-state properties, the two interacting **4** in the unit cell are used for the calculations (Figure 11).

The HOMO is composed primarily of the chlorine lone pair, Au d_{xy} and p orbital of the sulfur atom of the C═S bond (Figure 11). Some minor contributions of the remainder of the π system of the dithiolene ligand are also noted. The LUMO is now mainly composed of the π system of the trithiocarbonate part of the dithiolene. All in all, these computations indicate that the lowest energy transition is X/MLCT (i.e., halide/metal-to-ligand charge transfer). Such assignment is not unusual.[33] The computed transition wavelength is 425 nm, which compares favorably to that observed in the spectra (i.e., about 480 nm in the solid and 420 nm in solution; Figure 10). The fact that the emission maximum is red-shifted in the solid with respect to the solution is due to Au···Au interactions, generating sets of Au_2-centered bonding and antibonding orbitals as depicted by Forward and collaborators[2b] mixed with the MLCT manifolds. Indeed, the gold d_{xy} orbital calculated in the HOMO combines in the

(33) Piché, D.; Harvey, P. D. *Can. J. Chem.* **1994**, *72*, 705.

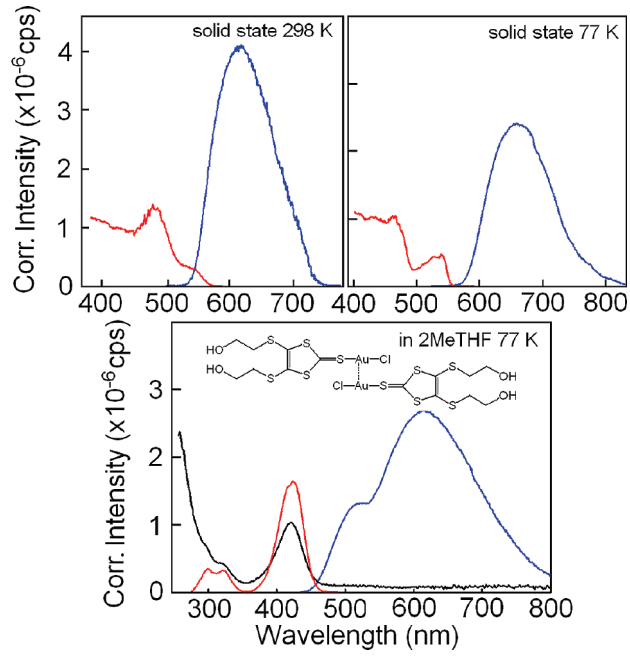

Figure 10. Emission (blue), excitation (red), and absorption spectra (black) of **4** in the solid state and in 2-MeTHF solution at 77 and 298 K. No luminescence was observed in solution at 298 K. The weak features at ~520 nm may be S_0-T_1 absorptions visible due to the large concentration (i.e., solid state) and the violation of the Beer−Lambert law.

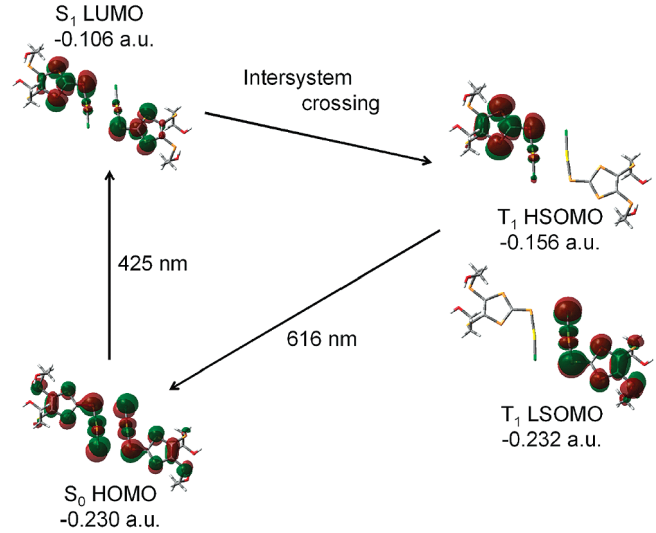

Figure 11. Calculated MOs involved in the absorption and emission spectra of two interacting complexes **4**.

dimer to form the dδ* contribution to the overall MO. So, we assign the MLCT transition for **4** in solution to an isolated complex, and for **4** in the solid state to a dimer-like, reminding the rotamers discussed for **1** and **2**. In the isolated state, **4** exhibits the HOMO and LUMO described in Figure 12.

The diradical nature of the triplet state consists of one electron of the LUMO on one complex **4** (−0.156 au) of the Au···Au interacting dimer and one electron located on the HOMO (−0.232 au) of the other complex **4**. The computed emission wavelength is 616 nm, which fits nicely with that observed at room temperature. Evidence for Au···Au interactions comes from the red-shift of the emission band which is expected upon contraction of the

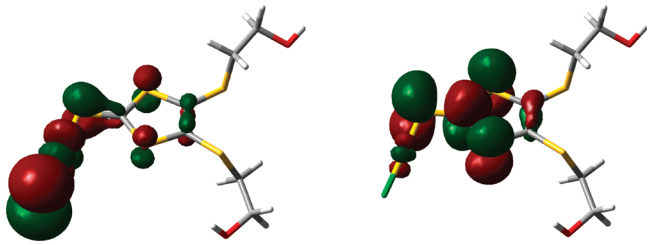

Figure 12. HOMO (left) and LUMO (right) of **4**. The calculations were performed on an optimized geometry of an isolated complex of [AuCl{$(HOCH_2CH_2)_2dmit$}].

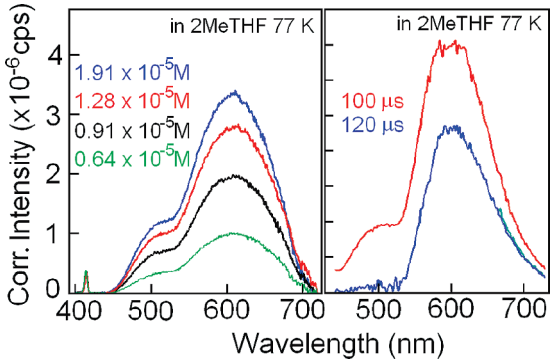

Figure 13. Left: Steady-state emission spectra of **4** at various concentrations showing no change in emission maximum nor the apparition of a new band. Right: Time-resolved emission spectra of **4** at two different delay times stressing evidence for two different species (fluorescence and phosphorescence).

unit cell (the crystal structure of **4** exhibits a Au···Au separation of 3.077 Å). **4** is not luminescent at 298 K. At 77 K, a strong emission band is observed with a maximum at ~ 610 nm, which is blue-shifted with respect to the solid-state emission spectrum (680 nm) at this temperature and to the one at 298 K (615). On the basis of this blue shift and the assignment made for the absorption band in solution, a MLCT assignment for an isolated molecule is also suggested. A study of the emission spectra as a function of the concentration was made (Figure 13). There was no change in emission maximum, illustrating that within the concentrations used in this work, the emission arises from an isolated molecule. A shoulder for which the relative intensity did not vary, exhibiting a different emission lifetime, was also noted for **4** in solution. From time-resolved spectroscopy on the nanosecond time scale (SI), the blue-shifted band decays in this same time frame. Because the excitation spectra are same for the red-shifted emission (i.e., phosphorescence), we assigned this blue-shifted band to fluorescence. The Stoke shift (i.e., energy gap between absorption and fluorescence) is indeed reasonable for this assignment (i.e., 3500 cm^{-1}). The emission lifetime is 1.38 ± 0.02 ns. This phenomenon was also reported by Eisenberg and his collaborators for other gold-containing materials.[34]

Conclusion

We synthesized two new members of dinuclear gold dithiolene complexes belonging to the type [{Au(PR_3)}$_2$(μ-1,2-dithiolene}]. The structural characterization reveals that the variation of the dithiolene residue has no major impact on the structural features compared with other literature-known examples, notably the Au···Au contacts remain in the range of about 3.1 Å. In contrast, upon treatment of AuCl(tht) with neutral five-membered thiones, the structural arrangement depends strongly on the nature of the organic ligands. In the case of the *Me_2dmit* ligand, no short gold contacts are encountered, whereas a surprisingly short unsupported aurophilic interaction is present in the dimeric [AuCl{$(HOCH_2CH_2)_2dmit$}]$_2$ complex. The presence of hydrogen bonding probably does not contribute to the dimerization (a similar dimeric motif has been observed using ethylene trithiocarbonate[27]), and the origin of the structural diversity remains to be explored. With this in mind, we are currently extending the reactivity of AuCl(tht) toward other sulfur-rich thiones. The photophysical studies revealed that the participation of intra- and intermolecular Au···Au interactions are relevant to the rich luminescent properties of these species. The nature of the excited states are essentially LMCT for the dithiolene derivatives **1** and **2** and X/MLCT for the thione compound **4**, where M could be an isolated Au unit or interacting Au···Au-containing species. In consequence, the emission spectra are strongly temperature-dependent. This phenomenon may be rationalized by a strengthening of the Au···Au interactions upon lowering the recording temperature.

Acknowledgment. Shawkat Mohammed Aly is thanked for the recording of emission and time-resolved spectra of **4** and *$(HOCH_2CH_2)_2dmit$*. The Besançon group thanks the regional council of the *Region de Franche-Comté* for funding of a spectrofluorimeter and the French Research Ministry for a Ph.D. grant for A. Hameau. The authors thank R. Eisenberg (University of Rochester) for fruitful discussion. The Natural Sciences and Engineering Research Council of Canada (NSERC) is acknowledged for funding. The work on compound **4** has been supported by the DFG (Deutsche Forschungsgemeinschaft) in the framework of SPP 1166.

Supporting Information Available: Representation of the supramolecular 2D network of **4** generated through intermolecular O−H···O bonding, the UV−vis spectra of *Me_2dmit* and **3**, time-resolved spectra of **4** in 2MeTHF at 77 K, and tables of selected computed transition energies by TDDFT. This material is available free of charge via the Internet at http://pubs.acs.org. Structures have been deposited with the Cambridge Crystallographic Data Centre (http://www.ccdc.cam.ac.uk; CCDC numbers: 663032 (**1**), 663031 (**2**), 663196 (**4**).

IC7022067

(34) Lee, Y.-A.; McGarrah, J. E.; Lachicotte, R. J.; Eisenberg, R. *J. Am. Chem. Soc.* **2002**, *124*, 10662.